

# Electronic Supplementary Information

## Monodispersed Copper Phosphide Nanocrystals in situ Grown into Nitrogen-doped Reduced Graphene Oxide Matrix and their Superior Performance as the Anode for Lithium-ion Batteries †

*Chenfeng Guo\*, Kai Pan, Ying Xie and Li Li*

*School of Chemistry and Materials Science, Key Laboratory of Functional Inorganic*

*Material Chemistry, Ministry of Education, Heilongjiang University, Harbin 150080,*

*People's Republic of China*

\* Corresponding author: Chenfeng Guo

E-mail: chenfengguo@hlju.edu.cn (Dr. Chenfeng Guo)

Tel: +86-451-86608545;

# 1 Experimental Section

## 2 Materials

3 Copper(II) chloride ( $\text{CuCl}_2$ , 99%) and 1-hexadecylamine (HDA, 90%) were obtained from Aladdin  
4 Industrial Corporation, China. 1-octadecene (ODE, 90 %), and Triphenyl phosphite (TPOP, 97%) were  
5 purchased from Alfa Aesar. Ethanol, n-hexane, graphite, sulfuric acid, urea, formamide, chloroform,  
6 hexafluorophosphoric acid ( $\text{HPF}_6$ ) and hydrogen peroxide were of analytical grade and obtained from  
7 various sources. All chemicals were used without further purification.

## 8 Materials synthesis

### 9 ***Cu<sub>3</sub>P@N-RGO Synthesis:***

10 Lyophilized GO was synthesized, as previously reported, with the modified Hummers method.<sup>[1]</sup> A  
11 procedure of “heating-up” was used for the synthesis of  $\text{Cu}_3\text{P@N-RGO}$  nanocomposites. The detailed  
12 process of preparation is as follows: in a three-necked flask of 50 mL was added the mixture of 0.05  
13 mmol (0.1279 g) of  $\text{CuCl}_2\cdot 2\text{H}_2\text{O}$ , 5.0 mmol (1.8110 g) of HDA, 5.0 mmol (2.3271 g) of TPOP, 10 g of ODE,  
14 5 mg urea and a suspension containing 35 mg of GO, which was magnetically stirred at room  
15 temperature under  $\text{N}_2$  flow. ( $\text{CuCl}_2$ : HDA: TPOP = 1:10:10) The mixed solution was, to some extent,  
16 cured before it was heated to 150 °C (5 °C/min) for an hour to remove ethanol. Then, the solution was  
17 kept in a vacuum for one hour to get rid of the remaining solvent with low-boiling point, moisture, and  
18 dissolved oxygen. Afterwards, the mixed solution was heated for half an hour to 260 °C (5 °C/min) under  
19 the protection of  $\text{N}_2$  flow. When the temperature of the solution dropped to 200 °C, the heat source  
20 was taken away and the solution was let to cool naturally to room temperature under the protection  
21 of  $\text{N}_2$  flow, too. As for the reaction solution, after it was transferred to a centrifuge tube, ethanol and  
22 n-hexane, both in a small amount, were added. In the next 15 minutes, the mixture was centrifuged at  
23 9000 rpm. After the precipitates were collected, 5 mL of ethanol and n-hexane were each added. When  
24 the precipitate became redispersed, another 20 mL of ethanol was added. Next, the product was  
25 collected through centrifugation. The precipitation and redispersion steps of the above procedure were  
26 repeated for 3 times. With the sample repeatedly washed and centrifuged, what was weakly bound on  
27 the nanocrystals surface almost got removed. At last, to complete the crystallization process of the  
28 sample, it took 6 hours for the  $\text{Cu}_3\text{P@N-RGO}$  nanocomposites to be dried at 60 °C, and 2 hours to be  
29 annealed at 350 °C in  $\text{N}_2$  atmosphere. By comparison,  $\text{Cu}_3\text{P}$  nanocrystals@RGO (abbreviated as  
30  $\text{Cu}_3\text{P@RGO}$ ) were manufactured in the same way with the preparation process of  $\text{Cu}_3\text{P@N-RGO}$   
31 without adding urea. N-RGO and RGO were manufactured by assembly of GO in the same hydrothermal  
32 way of synthesis with and without adding urea, respectively.<sup>[2]</sup>

### 33 ***Ligand exchange strategy:***

34 The organic ligand HDA was used to modify the surface of N-RGO and  $\text{Cu}_3\text{P}$ , which could result in  
35 the strong hydrophobic/hydrophobic interaction between them, hence, resulting in the uniform  
36 distribution of  $\text{Cu}_3\text{P}$  nanocrystals on N-RGO. The ligand exchange strategy we detailed here was used  
37 to displace organic ligands from the surface of  $\text{Cu}_3\text{P/N-RGO}$  nanocomposites, which is a key step toward  
38 their application in energy conversion and storage systems.

39 In brief, unreacted organic ligands were exchanged by mixing a new ligand ( $\text{HPF}_6$ ) in formamide,  
40 the 5 to 10 ml of a 0.05 to 0.1 M solution, with  $\text{Cu}_3\text{P@N-RGO}$  nanocomposites in chloroform, 10 ml of  
41 a solution (with concentration more or less equal to the crude solution). The preparation of the  $\text{HPF}_6$   
42 solution involved mixing formamide with aqueous  $\text{HPF}_6$  in corresponding amount (as received; ~63 wt. %  
43 in water). The mixture was stirred forcefully and set aside until the discovery of phase separation,

1 namely, Cu<sub>3</sub>P@N-RGO nanocomposites moving from the chloroform to the formamide phase. Fresh  
2 portions of chloroform were used to wash repeatedly the final formamide solution, which contained  
3 the Cu<sub>3</sub>P@N-RGO nanocomposites, to remove all the left organic ligands that surrounded the Cu<sub>3</sub>P@N-  
4 RGO nanocomposites. Hence, pure Cu<sub>3</sub>P@N-RGO nanocomposites were obtained, free of any organic  
5 ligands.

## 6 **Materials characterization**

7 The collected products were characteristic of the usage of powder XRD on a Rigaku diffractometer  
8 with Cu K $\alpha$  radiation. XPS (Kratos Axis ULTRA) was utilized in the analysis of the chemical compositions  
9 of the synthesized samples. A Tristar II 3020 instrument was used for measuring N<sub>2</sub> adsorption and  
10 desorption isotherms at 77K, and the method of the BET was applied to the measurement of the specific  
11 surface area. The calculations of pore diameter and pore size distribution were based on the BJH model.  
12 Thermo-Fischer Almega dispersive Raman instrument was used due to Raman measurements at room  
13 temperature, with its the excitation wavelength being 633 nm. As for the FTIR spectra, it was recorded  
14 with a spectrometer of Nicolet 5700 FTIR. The measurement of TG (Mettler Toledo TG/DSC1 STARE  
15 System) analysis was carried out, from room temperature up to 800 °C, with a heating rate of 10 °C  
16 min<sup>-1</sup> in air flow. To measure the electronic conductivity of samples at room temperature (SB120; San  
17 Feng), a conductivity test metre with four probes was used. Operated at 200 kV, JEM-3010 microscopes  
18 were used for the morphology and microstructure of the samples. Samples for the TEM and HRTEM  
19 were dealt with dispersion in ethanol, with sonication of scraped powders, which was dropped onto Cu  
20 grids coated with carbon. The usage of a high precision electronic balance (XP105DR, Mettler Toledo)  
21 was for tipping the scale at all the materials.

## 22 **Electrochemical Measurement**

### 23 ***Manufacturing Electrodes and Coining Cells:***

24 To manufacture the electrodes, the choice of active material was the as-obtained Cu<sub>3</sub>P@N-RGO  
25 and a mixture (slurry) was made up with polyvinylidene fluoride (PVDF) used as binder, N-methyl-2-  
26 pyrrolidone (NMP) used as solvent, carbon black used as conductor, with the mass ratio being 80:10:10  
27 (active material: PVDF: carbon black). The resultant slurries were pasted, as a current collector, on the  
28 Cu foil, which was cut into disks, after it was dried at 75 °C for 12 hours in a vacuum oven and  
29 compressed at a given pressure, with a diameter of 1.5 cm and an average loading mass of *ca.* 1 mg/cm<sup>2</sup>.  
30 An argon-filled glove box was used for the assembling of the CR2032-type half-cells, with the contents  
31 of O and moisture controlled under 1 ppm, and an electrolyte of 1 M of lithium hexafluorophosphate  
32 (LiPF<sub>6</sub>) in the solvent of ethylene carbonate (EC)/dimethyl carbonate (DMC)/diethyl carbonate (DEC)  
33 was used with a separator of Celgard 2500 (polypropylene), an anode of active material and a cathode  
34 of metal lithium disks.

### 35 ***Electrochemical Characterization:***

36 A Land (CT2001A) system was applied at room temperature, over a voltage range of 0.01-2.5 V (*vs.*  
37 Li/Li<sup>+</sup>), for the test of galvanostatically discharged and charged measurements of the cells. It should be  
38 noted that “n C” suggests setting up the discharge/charge current to get the nominal capacity in “1/n”  
39 hours. For the working Cu<sub>3</sub>P@N-RGO electrode, the weight of the material was applied to evaluate the  
40 specific discharge capacity of the cell, which was showed in mA<sub>h</sub>g<sup>-1</sup> of Cu<sub>3</sub>P@N-RGO. Based on the  
41 equation given below, an assumed capacity (Q) of the theoretical mixture of Cu<sub>3</sub>P@N-RGO could be  
42 calculated as follows:

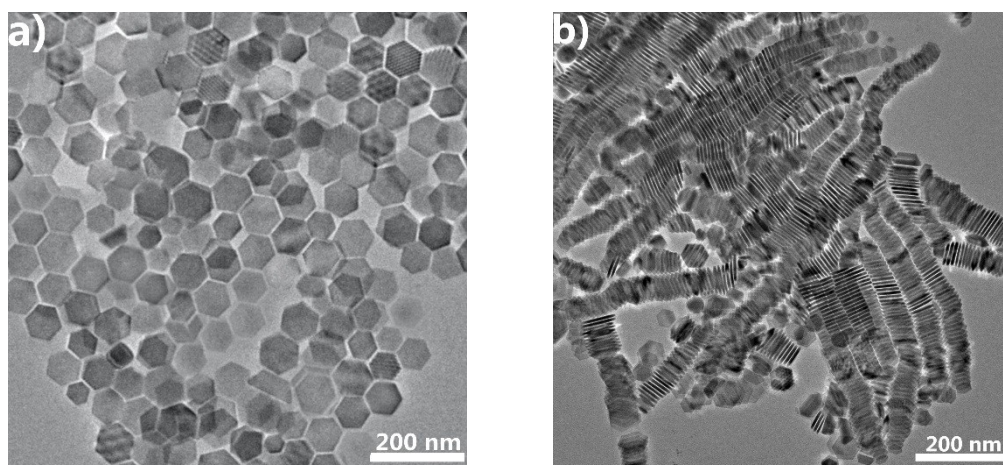
$$43 \quad Q_{\text{theoretical}} = Q_{\text{Cu}_3\text{P NPs}} \times \text{mass percentage of Cu}_3\text{P NPs} + Q_{\text{N-RGO}} \times \text{mass percentage of N-RGO}$$

1 
$$=363 \times 87.42\% + 372 \times 12.58\% = 364.13 \text{ mAh g}^{-1}$$

2 The collection of CV curves was based on a CHI660C electrochemistry workstation at  $0.1 \text{ mV}\cdot\text{s}^{-1}$   
3 between 0.01-3.0 V (vs. Li/Li<sup>+</sup>). As for the as-prepared anodes, their EIS was measured on a PARSTAT  
4 2273 electrochemical station over a frequency ranging 10 000 to 0.1 Hz with an amplitude of 5 mV. The  
5 experiments were repeated for verifying the recurrence of the electrochemical data, until another  
6 anode of the same specimen was at least obtained.

7  
8  
9  
10  
11  
12  
13  
14  
15  
16  
17  
18  
19  
20  
21  
22  
23  
24  
25  
26  
27  
28  
29  
30  
31  
32  
33  
34  
35  
36  
37  
38  
39  
40  
41  
42  
43  
44  
45

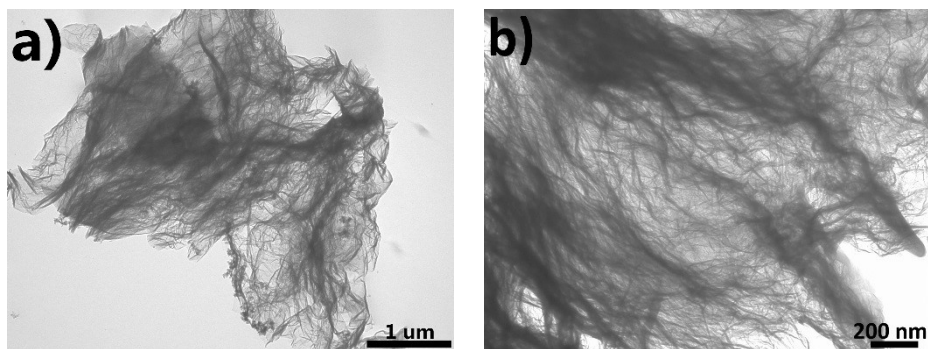
1 **S1. Morphology information of the as-prepared Cu<sub>3</sub>P nanocrystals.**



3 **Fig. S1†** (a) top-view TEM image of the as-synthesized Cu<sub>3</sub>P nanocrystals, showing Cu<sub>3</sub>P nanocrystals  
4 exhibited quasi-hexagonal plate-like shape and sizes tunable from 25 to 40 nm, as well as obvious  
5 irregular aggregation between Cu<sub>3</sub>P nanocrystals; (b) cross-view TEM image of the as-synthesized Cu<sub>3</sub>P  
6 nanocrystals, showing the forming of columnar stacks, as well as obvious irregular aggregation between  
7 Cu<sub>3</sub>P nanocrystals, too.

8  
9  
10  
11  
12  
13  
14  
15  
16  
17  
18  
19  
20  
21  
22  
23  
24  
25  
26  
27  
28  
29  
30  
31

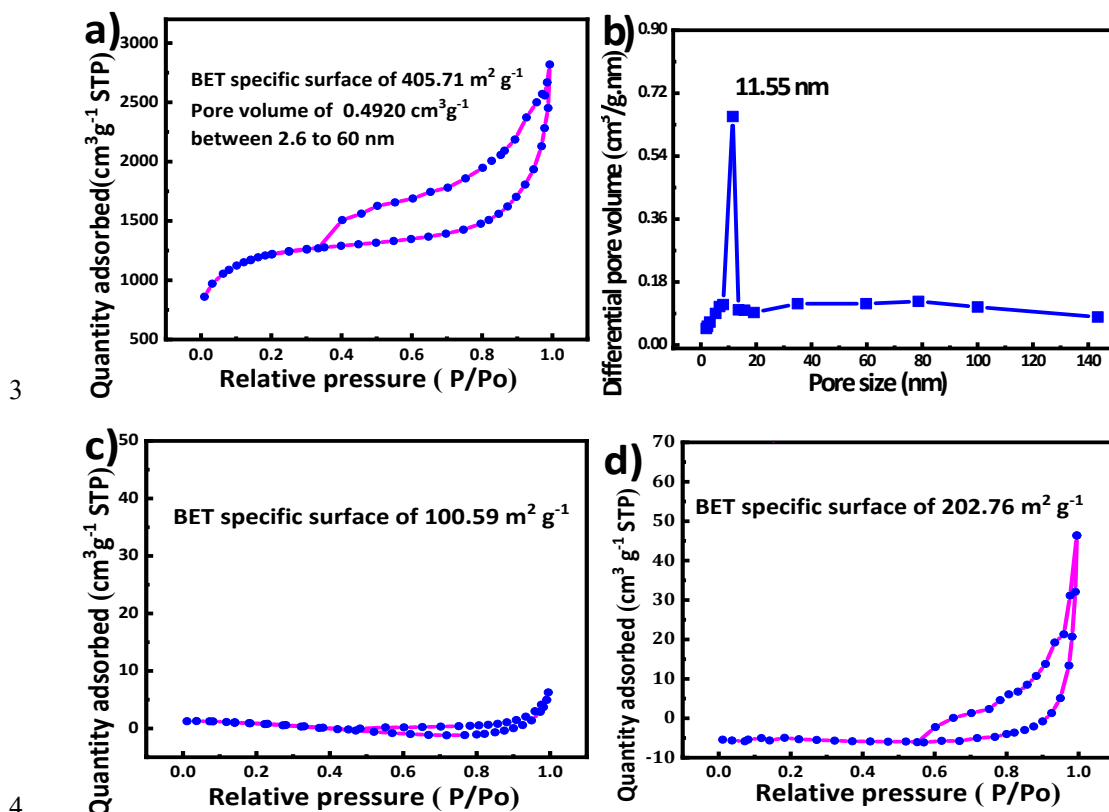
1 **S2. Morphology information of the as-prepared N-RGO.**



3 **Fig. S2†** TEM images of N-RGO at different magnifications: revealing 3D graphene network, completely  
4 interconnected and porous, with randomly opened hole nanostructure.

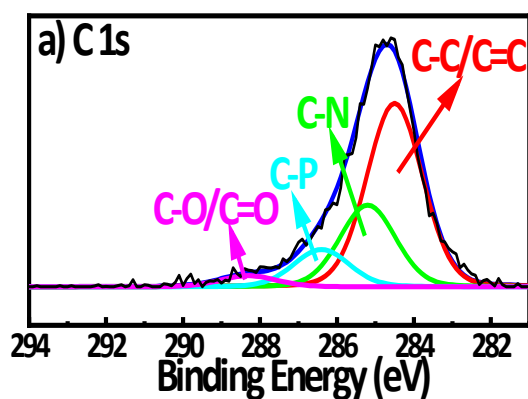
5  
6  
7  
8  
9  
10  
11  
12  
13  
14  
15  
16  
17  
18  
19  
20  
21  
22  
23  
24  
25  
26  
27  
28  
29  
30  
31  
32  
33  
34

1 **S3.** N<sub>2</sub> isothermal adsorption-desorption measurement of Cu<sub>3</sub>P@N-RGO  
2 nanocomposites, Cu<sub>3</sub>P nanocrystals and N-RGO matrix.



8  
9  
10  
11  
12  
13  
14  
15  
16  
17  
18  
19  
20  
21  
22  
23  
24  
25

1 **S4. XPS spectrum information of Cu<sub>3</sub>P@N-RGO nanocomposites.**



2

3 **Fig. S4†** High resolution XPS spectrum of C 1s for Cu<sub>3</sub>P@N-RGO nanocomposites. Four peaks at 284.5  
4 eV, 285.2 eV, 286.4eV and 288.3 eV were attributed to C-C/C=C, C-N, C-P and C-O/C=O bonds.

5

6

7

8

9

10

11

12

13

14

15

16

17

18

19

20

21

22

23

24

25

26

27

28

29

30

31

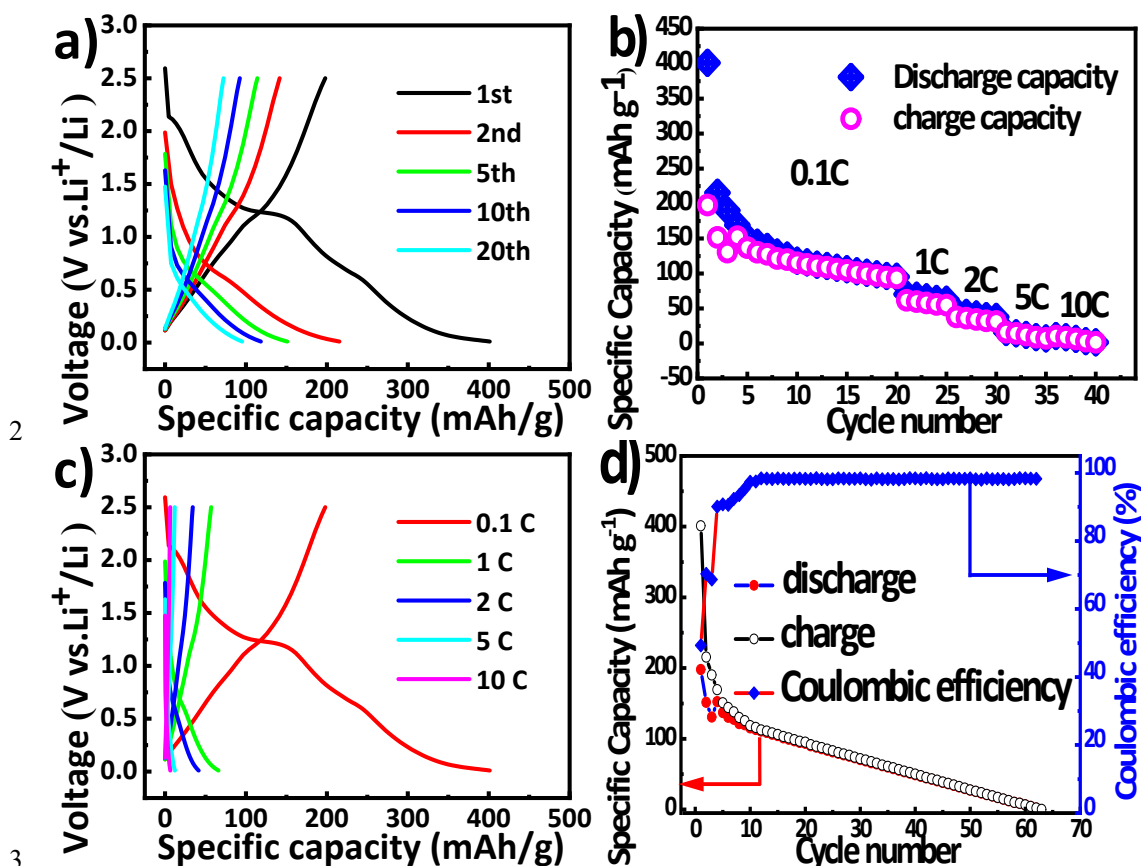
32

33

34



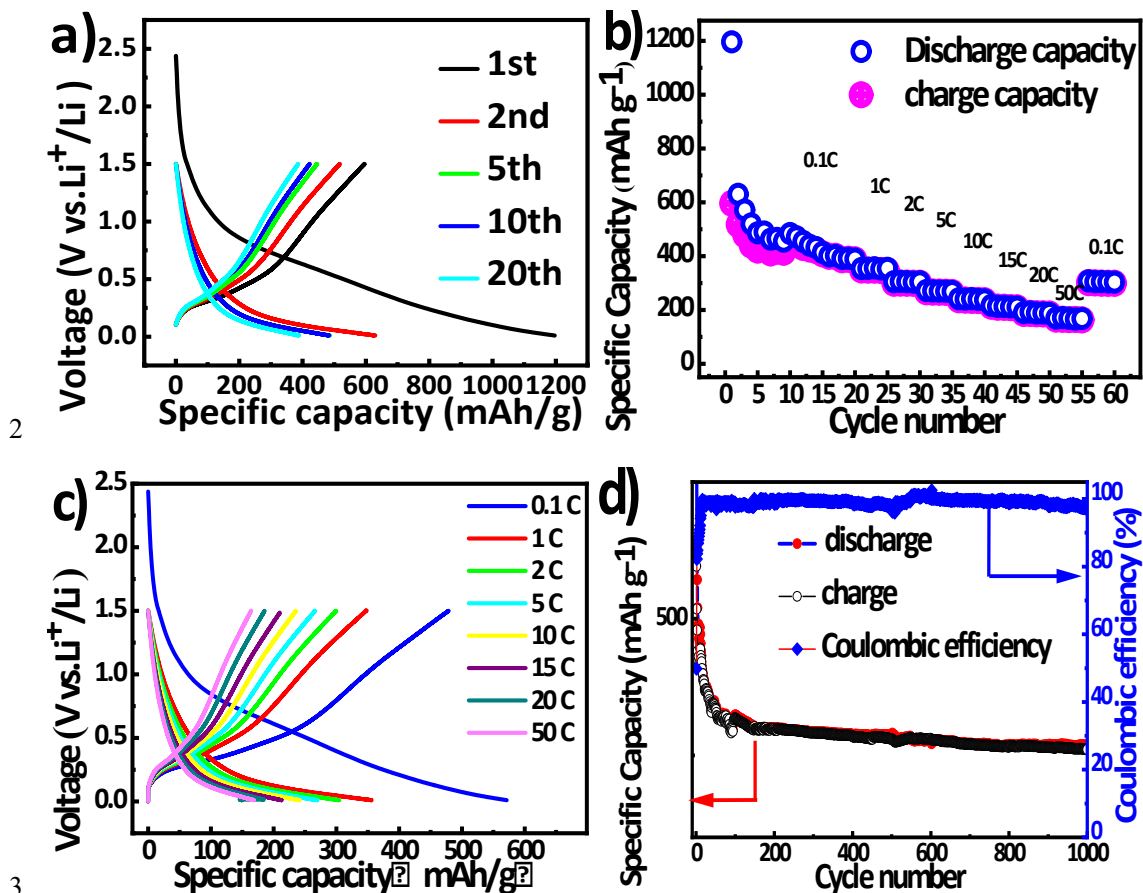
1 S5. Electrochemical performance of  $\text{Cu}_3\text{P}$  nanocrystals.



4 Fig. S5† Properties of  $\text{Cu}_3\text{P}$  nanocrystals in terms of Electrochemistry: (a) The profiles of discharge and  
 5 charge at 0.1 C for the cycles of the 1st, 2nd, 5th, 10th and 20th. With the initial Coulombic efficiency  
 6 being 49.3%, 401.2 and 197.9  $\text{mA h g}^{-1}$  are the capacities of the first discharge and charge, which are  
 7 based on the overall anode mass of  $\text{Cu}_3\text{P}$  nanocrystals. (b) rate performance cycled at 0.1 - 10 C. (c)  
 8 discharge and charge profiles at current rates of 0.1 - 10 C and (d) cycling performance at 0.1 C vs.  
 9 Coulombic efficiency:  $\text{Cu}_3\text{P}$  nanocrystals anode became un-rechargeable after 63 cycles under a current  
 10 rate of 0.1C, which indicates an inferior cycling performance.

11  
 12  
 13  
 14  
 15  
 16  
 17  
 18  
 19  
 20  
 21  
 22  
 23  
 24

1 S6. Electrochemical performance of N-RGO matrix.



4 Fig. S6† Properties of N-RGO matrix in terms of Electrochemistry: (a) The profiles of discharge and  
 5 charge at 0.1 C for the cycles of the 1st, 2nd, 5th, 10th and 20th. With the initial Coulombic efficiency  
 6 being 49.81%, 1196.4 and 596.0 mA h g<sup>-1</sup> are the capacities of the first discharge and charge, which are  
 7 based on the overall anode mass of N-RGO matrix. (b) rate performance cycled at 0.1 - 10 C. (c)  
 8 discharge and charge profiles at current rates of 0.1 - 10 C and (d) cycling performance at 0.1 C vs.  
 9 Coulombic efficiency: N-RGO matrix anode exhibits a charge capacity of 260.5 mA h g<sup>-1</sup> after 1000 cycles  
 10 under a current rate of 0.1C, which indicates a common cycling stability.

11  
 12  
 13  
 14  
 15  
 16  
 17  
 18  
 19  
 20  
 21  
 22

## 1 **References:**

- 2 [1] Xiong, Z.; Zhang, L.; Ma, J.; Zhao, X. Photocatalytic degradation of dyes over graphene-gold  
3 nanocomposites under visible light irradiation. *Chem. Commun.* **2010**, 46, 6099-6101.
- 4 [2] Guo, C.; Wang, D.; Liu, T.; Zhu J.; Lang, X. A three dimensional SiO<sub>x</sub>/C@ RGO nanocomposite as  
5 a high energy anode material for lithium-ion batteries. *J. Mater. Chem. A* **2014**, 2, 3521-3527.